Aerobic Oxidative Dehydrogenation of Coordinated Imidazoline Units of Pincer Ruthenium Complex

Shusaku Maeda[a], Take-aki Koizumi[a], Takakazu Yamamoto[a], Koji Tanaka[b], and Takaki Kanbara[c,d]*

[a] *Chemical Resources Laboratory, Tokyo Institute of Technology, 4259 Nagatsuta, Midori-ku, Yokohama, 226-8503, Japan*

[b] *Institute for Molecular Science, 5-1 Higashiyama, Myodaiji, Okazaki, Aichi 444-8787, Japan*

[c] *Tsukuba Research Center for Interdisciplinary Materials Science (TIMS), University of Tsukuba, 1-1-1 Ten-noudai, Tsukuba 305-8573, Japan*

[d] *Graduate School of Pure and Applied Sciences, University of Tsukuba, 1-1-1 Ten-noudai, Tsukuba 305-8573, Japan*

Corresponding author.

Tel.: +81-29-853-5066; fax: +81-29-853-4490; E-mail: kanbara@ims.tsukuba.ac.jp

Abstract

A new pincer ruthenium complex (**1**; $[RuL^1(tpy)](PF_6)$; L^1 = 1,3-di(2-imidazoline-2-yl)benzene, tpy = 2,2':6',2"-terpyridine) having a κ^3NCN pincer ligand with two imidazoline units and related ruthenium complexes were synthesized and characterized. The imidazoline units of **1** were oxidized in air to give an imidazole-ligated pincer complex (**2**; $[RuL^2(tpy)](PF_6)$; L^2 = 1,3-di(2-imidazolyl)benzene). Results of the ^{1}H NMR spectroscopic and cyclic voltammetric studies of the complexes indicate that the σ-donor character of the pincer ligand of **1** induces the Ru-promoted oxidative dehydrogenation of coordinated imidazoline moieties to imidazole units with oxygen in air.

Keywords: Ruthenium; Pincer ligand; Imidazoline; Imidazole; Oxidative dehydrogenation

1. Introduction

The oxidative dehydrogenation of coordinated amines and alcohols has been a subject of interest [1]. The reaction is promoted by the coordination of the substrates to the transition metal center; note that ruthenium and osmium are particularly effective oxidizing centers [1a]. Various ruthenium complexes with imidazoline ligands, including *N*-heterocyclic carbene complexes, have been prepared and utilized as catalysts [2]. However, to our knowledge, there has been no report on the metal-promoted oxidation of imidazoline ligands [3].

The oxidative dehydrogenation of imidazolines to imidazoles is biologically and pharmaceutically very important [4].

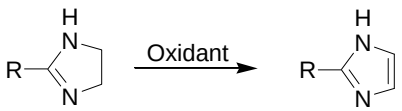

Most of the reported synthetic studies of imidazole derivatives, however, require toxic or explosive oxidants. We here report on synthesis, electrochemical properties, and reactivities of a new ruthenium complex (**1**) having

a κ^3NCN pincer ligand with two imidazoline units. **1** exhibits a unique oxidative dehydrogenation of the coordinated imidazoline moiety with aerial oxygen to give an imidazole-ligated pincer ruthenium complex (**2**). The reactivity of a related κ^3NNN tridentate ruthenium complex (**3**) and speculated oxidation process of **1** are also described.

2. Results and Discussion

The Ru complex **1** was prepared by reaction of $RuCl_3$(tpy) (tpy = 2,2':6',2"-terpyridine) with 2 equiv of $AgPF_6$ followed by *ortho,ortho*-cyclometalation of 1,3-di(2-imidazoline-2-yl)benzene (**4**) [5] in 2-methoxyethanol under N_2, whereas the imidazole-ligated complex **2** was obtained under the same reaction conditions in air (Scheme 1). **2** was considered to be produced by the oxidative dehydrogenation of imidazoline moieties of **1** with oxygen in air. In contrast, the related Ru complex **3** was prepared under similar conditions in both N_2 and air, as shown in Scheme 2 .

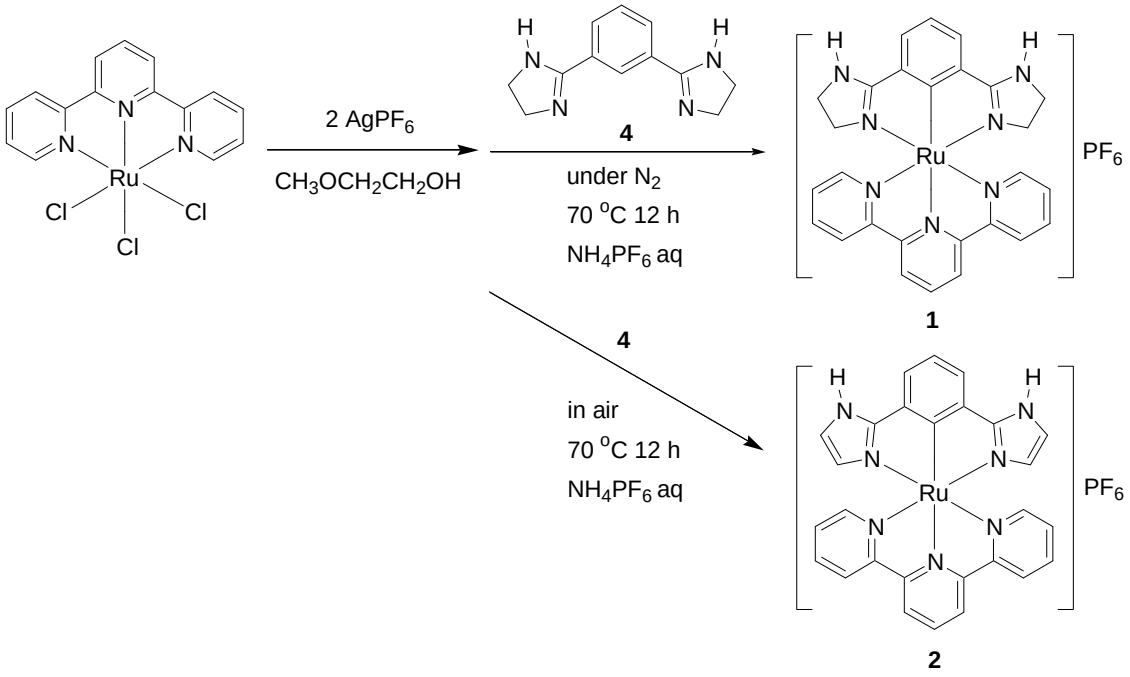

Scheme 1

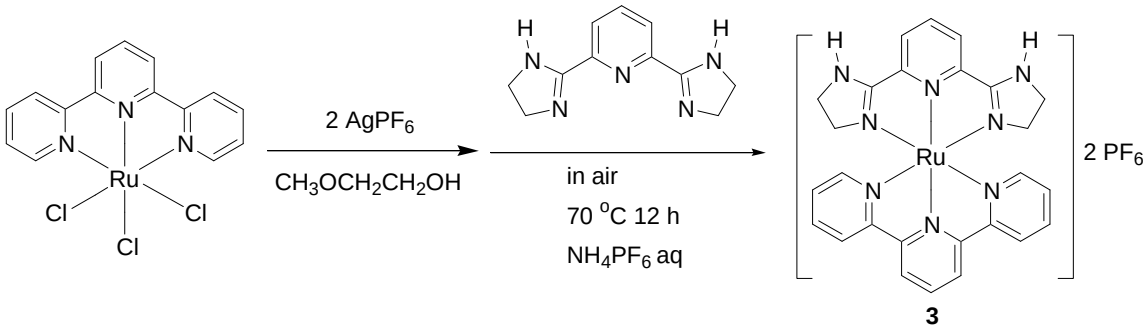

Scheme 2

The structures of the complexes **1**-**3** were confirmed by NMR spectroscopy and ESI-mass spectroscopy.

1 was stable in the solid state in air, however, the aerobic oxidation of **1** gradually proceeded in solutions at 70 °C, which was monitored by ^{1}H NMR spectroscopy; the results of which are shown in Fig. S1 in Supplementary material. A decrease in the intensity of the signals assigned to the 4,5-H of the imidazoline ring (δ 3.31 and 2.39) and the appearance of the signals assigned to the 4,5-H of the imidazole ring (δ 6.68 and 5.71) were observed, and the conversion reached approximately 100% after 9d. In the oxidation experiments, the intermediate complex **5** (*m/z* = 546) was detected by ESI-mass spectroscopy, indicating the successive oxidative dehydrogenation of the imidazoline moieties of **1**. The oxidation of **1** was considerably accelerated by the addition of a base such as KO-*tert*-Bu. In contrast, **3** was fairly stable in solution even in air for weeks. These results indicate that the presence of the Ru-C_{ipso} σ-bond of **1** induces the aerobic oxidation of the ligated imidazoline to imidazole moieties [6].

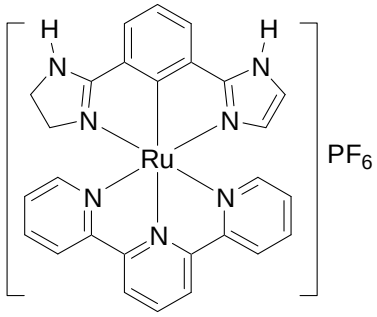

5

The ORTEP drawing of **1** is shown in Figure 1. **1** has distorted octahedral geometries similar to that of $[Ru(tpy)_2]^{2+}$ [7], and the Ru-C and Ru-N bond lengths of **1** are in the range of those of related pincer Ru complexes [8]. The ORTEP drawings of **2**, **3**, and **5** and detailed results of X-ray crystallography of the complexes are shown in Fig. S2 and Table S1 in Supplementary material [9].

The electrochemical data of **1**-**3** are summarized in Table 1. **1** exhibited three reversible redox couples at $E_{1/2}$ = - 2.01 V, -0.15 V, and 0.79 V (versus Ag^+/Ag) in acetonitrile under N_2. Owing to the σ-donor character of the pincer ligand [10], the metal-centered oxidation of **1** (Ru(II)/Ru(III); $E_{1/2}$ = -0.15 V versus Ag^+/Ag) occurred at a lower oxidation potential than that of **3** by 0.59 V. The metal-centered redox couple of **1** essentially remained unchanged for repeated scans under N_2, and no electrochemical response occurring at the ligand of **1** was observed in the scan range. In contrast, the aerobic chemical transformation of **1** proceeded in methanol solution at 55 °C as shown in Figure 2. After stirring the solution at 55 °C for 72 h in air, the metal-centered redox couple of **1** (observed at –0.10 V in Figure 2(b)) was reduced and a new redox couple appeared at 0.02 V. The new redox couple is associated with the Ru(II)/Ru(III) response of **2**. When a similar heat treatment of **1** was carried out under N_2, the electrochemical behavior showed no change, whereas electrolysis of **1** at 0.1 V for 24 h under N_2 caused the consecutive oxidation of the ligated imidazoline moieties of **1**; the electrochemical response of **2** ($E_{1/2}$ = -0.05 V) was observed. **3** was fairly stable under the aerobic heat treatment that it gave the same voltammogram.

The oxidative dehydrogenation of the ligated imidazoline units of **1** is reminiscent of the metal-promoted oxidation of coordinated amines to imines [1]. Goswami *et al*. reported the

ruthenium-promoted oxidative chemical transformation of coordinated ligands [11]. On the basis of the present results, a plausible reaction mechanism for the ruthenium-promoted imidazoline-to-imidazole oxidation with oxygen in air is shown in Scheme 3. The oxidation requires two deprotonation steps from the coordinated imidazoline unit. The electron donating ability of the pincer ligand of **1** facilitates the initial oxidation of the Ru(II) center of **1** with oxygen in air to form the Ru(III) intermediate; this is consistent with the results of cyclic voltammetric studies. Then, the ligated imidazoline units undergo oxidative dehydrogenation; consecutive intramolecular electron transfer from the uncoordinated amine nitrogen atom to the Ru(III) metal center through the conjugation of imidazoline moieties is considered to lead to deprotonation. The formation of 1H-imidazole involves tautomerizing 4H-imidazole. The postulated pathway coincides with the fact that oxidation is accelerated under basic conditions. On the other hand, Taube *et al*. have proposed that 2Ru(III) → Ru(II) + Ru(IV) disproportionation occurs under basic conditions in ruthenium complexes containing dissociable protons [1a,c]. Therefore, an alternative two-electron transfer pathway involving such disproportionation to form a Ru(IV) species is also postulated (Scheme 4). However, the two pathways have little difference because the Ru(IV) intermediate is considered to include a contribution from the resonance structure as shown in Scheme 5.

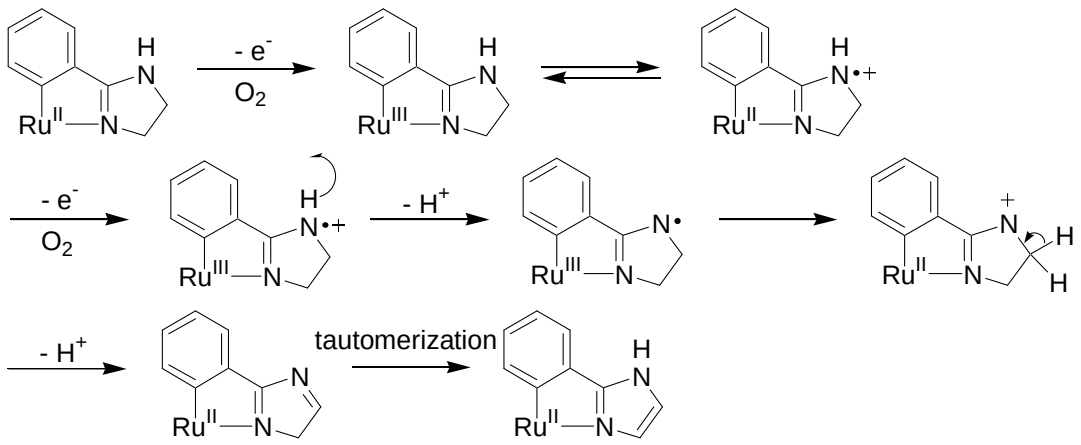

Scheme 3 Plausible reaction pathway of aerobic oxidative dehydrogenation of ligated imidazoline units of **1**

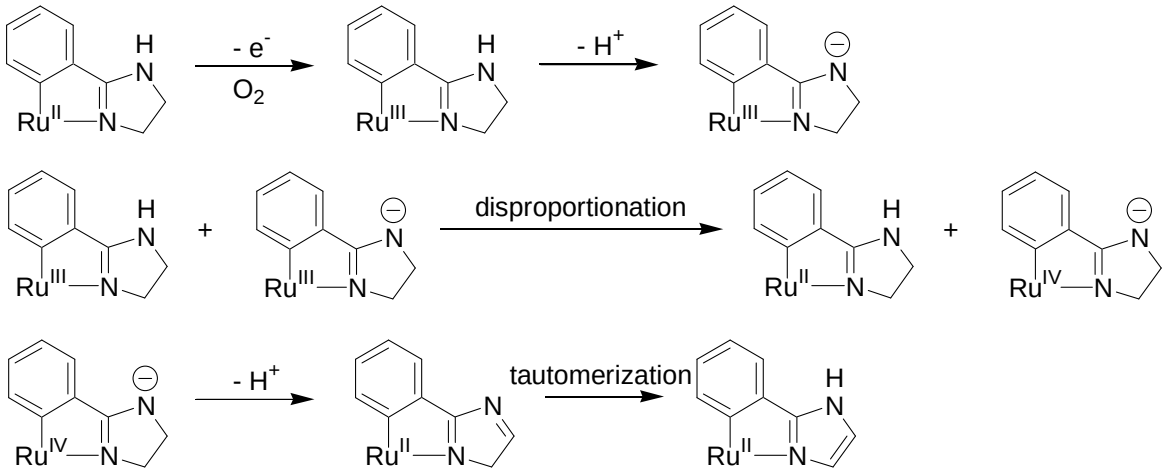

Scheme 4 Alternative reaction pathway

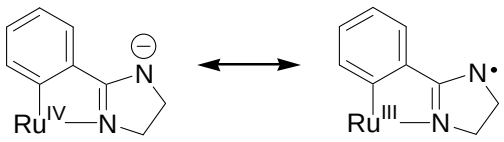

Scheme 5

As described above, the κ^3NCN pincer ruthenium complex **1** undergoes a unique chemical transformation with oxygen in air to produce **2**. This is the first example showing that the electron donating nature of the pincer ligand facilitates the ruthenium-promoted oxidation of a ligated imidazoline moiety.

3. Experimental

3.1. General procedures and materials

Solvents for the reactions and measurements were dried and distilled prior to use. The ligands, 1,3-di(2-imidazoline-2-yl)benzene (**4**) [5], 2,6-di(2-imidazoline-2-yl)pyridine [12], and $RuCl_3$(tpy) [13] were prepared as described previously.

*3.2. Preparation of Ru complexes (**1**-**3**)*

1: $RuCl_3$(tpy) (100 mg, 0.23 mmol) was dissolved in 2-methoxyethanol (20 ml), and $AgPF_6$ (115 mg, 0.45 mmol) was added. The reaction mixture was stirred at 70 °C for 2 h under N_2. After the Ag salt was filtered off, the solution was degassed by three cycles of the freeze-thaw procedure under N_2. **4** (50 mg, 0.23 mmol) was added to the solution, and the solution was stirred at 70 °C for 12 h under N_2. The purple solution was concentrated to *ca*. 1 ml, and poured into an aqueous NH_4PF_6 solution. The purple precipitate was collected by filtration and purified by column chromatography with almina to give a purple powder of **1** (21 mg, 13% yield).

1: ESI-mass: m/z = 548 $[M\text{-}PF_6]^+$. HI-ESI-mass: calcd for $C_{27}H_{24}N_7Ru$: 548.1137. Found: 548.1144. ^{1}H NMR (400 MHz in CD_3CN): δ 8.50 (d, *J*= 7.86 Hz, 2H), 8.27 (d, *J*= 7.86 Hz, 2H), 7.95 (t, *J*= 7.97,1H), 7.69 (d, *J*= 7.53 Hz, 2H), 7.65 (td, *J*= 7.55 Hz, *J*= 1.95 Hz, 2H), 7.25 (t, *J*= 7.50 Hz, 1H), 7.08-7.00 (m, 4H), 6.17 (s, 1H), 3.31 (t, *J*= 9.62 Hz, 4H), 2.39 (t, *J*= 9.17 Hz, 4H). $^{13}C\{^1H\}$ NMR (100 MHz in CD_3CN): δ 175.5, 160.1, 154.8, 154.0, 134.2, 130.0, 126.7, 124.9, 122.7, 121.7, 119.8, 118.2, 51.6, 45.9.

2 was prepared analogously in air.

2: 20% yield. ESI-mass: m/z = 544 $[M\text{-}PF_6]^+$. HI-ESI-mass: calcd for $C_{27}H_{20}N_7Ru$: 544.0824. Found: 544.0831. ^{1}H NMR (400 MHz in CD_3CN): δ11.03 (s, 2H), 8.58 (dd, *J*= 8.04 Hz, *J*= 1.96, 2H), 8.30 (dd, *J*= 8.00 Hz, *J*= 0.62 Hz, 2H), 8.05 (td, *J*= 7.93, *J*= 1.95 Hz, 1H), 7.86 (d, *J*= 7.56 Hz, 2H), 7.60 (td, *J*= 7.82 Hz, *J*= 1.05, 1H), 7.31 (td, *J*= 7.57 Hz, *J*= 1.69, 2H), 7.13 (dd, *J*= 5.60 Hz, *J*= 0.72 Hz, 2H), 6.93 (td, *J*= 6.47 Hz, *J*= 1.00 Hz, 2H), 6.68 (d, *J*= 1.24 Hz, 2H), 5.71 (d, *J*= 1.00 Hz, 2H). $^{13}C\{^1H\}$ NMR (100 MHz in CD_3CN): δ 166.3, 160.5, 157.5, 155.0, 134.8, 134.5, 130.8, 128.6, 126.7, 123.2, 122.0, 120.8, 120.3, 116.7.

3 was prepared analogy with **2** using 2,6-di(2-imidazoline-2-yl)pyridine.

3: 22% yield. ESI-mass: m/z = 275 $[M\text{-}PF_6]^{2+}$. HI-ESI-mass: calcd for $C_{26}H_{24}N_8Ru/2$: 275.0584. Found: 275.0582. ^{1}H NMR (400 MHz in CD_3CN): δ 8.57 (d, *J*= 8.04, 2H), 8.40 (d, *J*= 7.68 Hz, 2H), 8.30-8.16 (m, 4H), 7.94 (td, *J*= 7.88 Hz, *J*= 1.47, 2H), 7.30 (td, *J*= 6.59 Hz, *J*= 1.35, 2H), 7.19 (dd, *J*= 5.58 Hz, *J*= 0.83, 2H), 6.94 (s,

1H), 3.54 (td, *J*= 10.5, *J*=1.35, 4H), 2.71 (t, *J*= 10.4, 4H). $^{13}C\{^{1}H\}$ NMR (100 MHz in CD_3CN): δ 167.8, 158.8, 156.2, 153.3, 149.1, 138.0, 135.7, 135.1, 128.2, 125.5, 124.0, 123.4, 52.4, 46.0.

*3.3 Crystal data for **1, 2, 3, and 5***

The diffraction data were collected with a Rigaku Saturn CCD area detector with graphite monochromated MoKα (λ = 0.71070 Å) at –160 ºC. The data were corrected for Lorentz and polarization effects, and an empirical absorption correction was applied. The structure was solved by direct methods (SIR 92) and expanded using Fourier techniques. The non-hydrogen atoms were refined anisotropically. Some hydrogen atoms were refined isotropically and the rest were refined using the riding model. X-ray crystallographic data for **1**-**3**, and **5** are summarized in Table S1 in Supplementary material. Despite several attempts, X-ray quality single crystals of **2** could not be obtained.

4. Supplementary material

Crystallographic data for the structural analysis have been deposited with the Cambridge Crystallographic Data Center; publication numbers CCDC 653741 (**1**·0.5MeCN), 653742 (**2**·1.5Et_2O), 653743 (**3**), and 653744 (**5**).

Figures giving time course of ^{1}H NMR spectrum of **1** in air, the ORTEP drawings of **2**, **3** and **5**, cyclic voltammograms of **1** and **3** in acetonitrile under N_2, and a table giving detailed results of X-ray crystallography of **1**, **2**, **3** and **5** are provided as Supplementary material. Supplementary data associated with this article can be found, in the online version, at doi:10.1016/j.jorganchem.2007.08.026.

Acknowledgement

The authors are grateful to Dr. R. Okamura, and Ms. K Tsutsui of Institute for Molecular Science for ESI-MS measurement.

References

[1] (a) F. R. Keene, Coord. Chem. Rev. 187 (1999) 121 and references therein. (b) S.-I. Murahashi, N. Komiya, Catalysis Today 41 (1998) 339 and references therein. (c) D. P. Rudd, H. Taube, Inorg. Chem. 10 (1971) 1543. (d) J. Gómez, G. García-Herbosa, J. V. Cuevas, A. Arnáiz, A. Carbayo, A. Muňoz, L. Falvello, P. E. Fanwick, Inorg. Chem. 45 (2006) 2488. (e) G. R. A. Adair, J. M. J. Williams, Tetrahedron Lett. 46 (2005) 8233. (f) S. Iwasa, K. Morita, K. Tajima, A. Fakhruddin, H. Nishiyama, Chem. Lett. (2002) 284. (g) M. Lee, S. Ko, S. Chang, J. Am. Chem. Soc. 122 (2000) 12011. (h) S. Medici, M. Gagliardo, S. B. Williams, P. A. Chase, S. Gladiali, M. Lutz, A. L. Spek, G. P. M. Klink, G. van Koten, Helvetica Chim. Acta 88 (2005) 694.

[2] (a) S. Bhor, G. Anikumar, M. K. Tse, M. Klawonn, C. Döbler, B. Bitterlich, A. Grotevendt, M. Beller, Org. Lett. 7, 2005, 3393. (b) I. Özdemir, B. Çetinkaya, S. Demir, E. Çetinkaya, N. Gürbüz, M. Çicek, Appl. Organomet. Chem. 18 (2004) 15. (c) C. Çetinkaya, B. Alici, I. Özdemir, C. Bruneau, P. H. Dixneuf, J. Organomet. Chem. 575 (1999) 187. (d) M. Scholl, S. Ding, C. W. Lee, R. H. Grubbs, Org. Lett. 1 (1999) 953. (e) J. A. Love, J. P. Morgan, T. M. Trnka, R. H. Grubbs, Angew. Chem. Int. Ed. 41 (2002) 4035.

[3] C. Sinha and coworkers have recently reported reduction of ligated imidazole unit to imidazoline in the osmium-carbonyl complex by $NaBH_4$; T. K. Mondal, T. Mathur, A. M. Z. Slawin, J. D. Woolins, C. Sinha, J. Ornanomet. Chem. 692 (2007) 1472.

[4] (a) M. Ishihara, H. Togo, Synlett (2006) 227. (b) A. de la Hoz, Á. Díaz-Ortiz, M. del C. Mateo, M. Moral, A. Moreno, J. Elguero, C. Foces-Foces, M. L. Rodríguez, A. Sánchez-Migallón, Tetrahedron 62 (2006) 5868. (c) I. Mohammadpoor-Baltork, M. A. Zolfigol, M. Abdollahi-Albeik, Tetrahedron Lett. 45 (2004) 8687. (d) K. C. Nicolaou, C. J. N. Mathison, T. Montagnon, J. Am. Chem. Soc. 126 (2004) 5192. (e) K. C. Nicolaou, C. J. N. Mathison, T. Montagnon, Angew. Chem. Int. Ed. 42 (2003) 4077. (f) M. Anastassiadou, G. Baziard-Mouysset, M. Payard, Synthesis (2000) 1814.

[5] (a) A. Kraft. J. Chem. Soc., Perkin Trans. 1 (1999) 705. (b) X.-Q. Hao, J.-F. Gong, C.-X. Du, L.-Y. Wu, Y.-J. Wu, M.-P. Song, Tetrahedron Lett. 47 (2006) 5033.

[6] The electron-withdrawing effect of pyridine unit of **3** may be the secondary reason for the inertness of the imidazoline moieties of **3**.

[7] (a) K. Lashgari, M. Kritikos, R. Norrestam, T. Norrby, Acta Cryst. C55 (1999) 64. (b) S. Pyo, E. Pérez-Cordero, S. G. Bott, L. Echegoyen, Inorg. Chem. 38 (1999) 3337.

[8] (a) C. M. Hartshorn, P. J. Steel, Organometallics, 17 (1998) 3487. (b) J.-P. Sutter, S. L. James, P. Steenwinkel, T. Karlen, D. M. Grove, N. Veldman, W. J. J. Smeets, A. L. Spek, G. van Koten, Organometallics 15 (1996) 941. (c) M. Gagliardo, H. P. Dijkstra, P. Coppo, L. De Cola, M. Lutz, A. L. Spek, G. P. M. van Klink, G. van Koten, Organometallics 23 (2004) 5833. (d) P. Dani, T. Karlen, R. A. Gossage, W. J. I. Smeets, A. L. Spek, G. van Koten, J. Am. Chem. Soc. 119 (1997) 11317.

[9] The X-ray quality single crystals of the intermediate complexes **5** were fortunately found during the oxidation experiments of **1**. Therefore, other identification of **5** except for ESI-MS could not be obtained.

[10] (a) S. Ott, M. Borgström, L. Hammarström, O. Johansson, Dalton Trans. (2006), 1434. (b) A. D. Ryabov, V. S. Sukharev, L. Alexandrova, R. L. Lagadec, M. Pfeffer, Inorg. Chem. 40 (2001) 6529.

[11] (a) P. Majumdar, L. R. Falvello, M. Tomás, S. Goswami, Chem. Eur. J. 7 (2001) 5222. (b) C. Das, A. Saha, C.-H. Hung, G.-H. Lee, S.-M. Peng, S. Goswami, Inorg. Chem. 42 (2003) 198. (c) P. Banerjee, G. Mostafa, A. Castiñeiras, S. Goswami, Eur. J. Inorg. Chem. (2007) 412.

[12] A. T. Baker, S. Singh, V. Vignevich, Aust. J. Chem. 44 (1991) 1041.

[13] S. J. Stoessel, C. M. Elliott, J. K. Stille, Chem. Mater. 1 (1989) 259.

Captions of Figures

Figure 1. X-ray crystal structure of **1** with thermal ellipsoids drawn at the 50% probability level. One of the four crystallographically independent molecules of **1** is shown. Hydrogen atoms, PF_6^- anions, and solvated acetonitrile molecules are omitted for simplicity.

Selected bond lengths (Å) and angles (deg): Ru1-C1, 1.969(6); Ru1-N1, 2.079(5); Ru1-N3, 2.084(5); Ru1-N5, 2.075(4); Ru1-N6, 2.022(5); Ru1-N7, 2.055(4); C8-C9, 1.527(10); C11-C12, 1.522(11); N1-Ru1-N3, 153.6(2); N5-Ru1-N7, 156.1(2); N6-Ru1-C1, 177.8(2).

Figure 2. Cyclic voltammograms of **1** (1.0 mM) in methanol containing $[(n\text{-Bu})_4N][PF_6]$ (0.1 M) under N_2 atmosphere: (a) before aerobic heat treatment and (b) after aerobic treatment at 55 ºC for 72 h. Sweep rate = 50 mV s^{-1}.

Figure S1 Time course of ^1H NMR spectrum of **1** in CD_3CN at 70 °C in air. A peak marked with an asterisk * is due to solvated water.

Figure S2 X-ray crystal structures of (a) **2** (b) **3**, and (c) **5** with thermal ellipsoids drawn at the 50% probability level. One of the two crystallographically independent molecules of **2** and one of the two crystallographically independent molecules of **5** are shown. Hydrogen atoms and PF_6^- anions and solvated ether molecules are omitted for simplicity.

Selected bond lengths (Å) and angles (deg):

(a) Ru1-C1, 2.008(6); Ru1-N1, 2.100(7); Ru1-N3, 2.084(7); Ru1-N5, 2.071(7); Ru1-N6, 1.998(7); Ru1-N7, 2.067(6); C8-C9, 1.320(13); C11-C12, 1.357(12); N1-Ru1-N3, 155.2(2); N5-Ru1-N7, 155.5(2); N6-Ru1-C1, 179.1(3).

(b) Ru1-N1, 2.004(3); Ru1-N2, 2.070(3); Ru1-N4, 2.070(2); Ru1-N5, 1.972(4); C5-C6, 1.512(7); N2-Ru1-N2*, 155.23(11); N4-Ru1-N4*, 158.11(11); N1-Ru1-N5, 0.0.

(c) Ru1-C1, 1.988(4); Ru1-N1, 2.099(3); Ru1-N3, 2.084(2); Ru1-N5, 2.068(3); Ru1-N6, 2.009(3); Ru1-N7, 2.055(2); C8-C9, 1.376(7); C11-C12, 1.468(7); N1-Ru1-N3, 154.18(12); N5-Ru1-N7, 156.53(13); N6-Ru1-C1, 174.24(13).

Figure S3 Cyclic voltammograms of (a) **1** and (b) **3** (1.0 mM) in CH_3CN containing $[(n\text{-Bu})_4N][PF_6]$ (0.1 M) under N_2. Sweep rate = 50 mV s^{-1}.